PeerJ Computer Science

Development of a novel machine learning framework for sustainable agricultural development

Abdu Salam[1,*], Fahd M. Aldosari[2], Gyu Sang Choi[3], Donia Y. Badawood[4], Isabel de la Torre[5], Roberto Marcelo Alvarez[6], Yini Miró[6] and Farhan Amin[3,*]

[1] Department of Computer Science, Abdul Wali Khan University, Mardan, Pakistan
[2] Department of Computer and Networks Engineering, Umm Alqura University, Makkah, Saudi Arabia
[3] School of Computer Science and Engineering, Yeungnam University, Gyeongsan, Republic of South Korea
[4] Department of Data Science, Umm Alqura University, Makkah, Saudi Arabia
[5] Department of Signal Theory and Communications, University of Valladolid, Valladolid, Spain
[6] Engineering Research & Innovation Group, Universidad Europea del Atlántico, Santander, Spain
* These authors contributed equally to this work.

ABSTRACT

To ensure the sustainable development of agriculture, the vegetation and water resources must be monitored accurately in the context of a changing climate. Spatial resolution, however, is a limitation of conventional satellite-based remote sensing methods, and they may not be able to detect the fine-scale patterns of agricultural activity in areas with low water availability. The integrated framework of multisensor remote sensing with super-resolution image enhancement for detecting agriculture and groundwater (GW) conditions in the Al Qassim region of Saudi Arabia is presented. Landsat, Gravity Recovery and Climate Experiment (GRACE), PlanetScope, and Climatic Research Unit Time-Series (CRU-TS) climate data were combined to assess the vegetation indices (VIs) Normalized Difference Vegetation Index (NDVI), Soil-Adjusted Vegetation Index (SAVI), Modified Soil-Adjusted Vegetation Index (MSAVI2), and their associations with temperature, rainfall, and groundwater storage (GWS). Three image enhancement techniques were considered, such as Bicubic interpolation, Super-Resolution Convolutional Neural Network (SRCNN), and the Super-Resolution Generative Adversarial Network (SRGNN)-based super-resolution model. The SRGAN model had the smallest root mean square error (RMSE) of 8.27 image intensity units in the 0–255 scaled reflectance space, and the highest peak signal-to-noise ratio (PSNR) and structural similarity index (SSIM) scores of 36.48 and 0.935, respectively. The results indicate that there is clear seasonal and annual variability in the vegetation indices, and there is a relationship between the vegetation condition at the regional scale and the climate variables, such as temperature, rainfall, and GWS. Spatial analysis also suggests that responses to vegetation and GW are not the same throughout the study area, due to the variable nature of agriculture, water availability, and climatic stresses encountered locally. The results show that SRGAN can enhance the spatial interpretability of the multi-sensor remote sensing imagery (RSE) and aid in climate-resilient monitoring of agriculture and water resource management.

Submitted 28 March 2026
Accepted 13 July 2026
Published 28 October 2026

Corresponding authors
Gyu Sang Choi, castchoi@yu.ac.kr
Farhan Amin, farhanamin10@hotmail.com

Academic editor
Kamran Shaukat

Additional Information and Declarations can be found on page 26

DOI 10.7717/peerj-cs.4071

Copyright
2026 Salam et al.

Distributed under
Creative Commons CC-BY 4.0

OPEN ACCESS

How to cite this article Salam A, Aldosari FM, Choi GS, Badawood DY, Torre Idl, Alvarez RM, Miró Y, Amin F. 2026. Development of a novel machine learning framework for sustainable agricultural development. PeerJ Comput. Sci. 12:e4071 DOI 10.7717/peerj-cs.4071

Subjects Artificial Intelligence, Computer Vision, Data Mining and Machine Learning, Spatial and Geographic Information Systems, Neural Networks
Keywords Machine learning, Deep learning, Image analysis, Sustainable agriculture, Super-resolution, Remote sensing

INTRODUCTION

Precise, timely, and spatially resolved data on vegetation health, irrigation requirements, land use transformation, and groundwater (GW) availability are becoming crucial for the sustainable development of agricultural systems (*Flora, 2010*). In arid and semi-arid agricultural areas, water scarcity and high evapotranspiration, as well as climate variability, have a direct impact on the productivity of the crops, and therefore on resource planning (*Yateh et al., 2025*). The monitoring of these variables with satellite technology (remote sensing) is a practical option for monitoring variables over large areas, but many satellite products available for free have spatial resolution issues that limit their application to agriculture for field-scale assessments (*Wu & Li, 2009*). GW irrigation is critical to agriculture in areas like Al Qassim in Saudi Arabia. So, it is very important to have reliable monitoring of the condition of vegetation and water availability for sustainable planning of agriculture. In addition to the Landsat imagery, there are also long-term observations of multispectral imagery, support for analysis of groundwater storage (GWS) with the Gravity Recovery and Climate Experiment (GRACE) mission, high spatial resolution reference imagery with the PlanetScope, and long-term climate variables with Climatic Research Unit Time-Series (CRU-TS). Integrated analysis is, however, not easy because the spatial resolution of these datasets varies (*Park, Park & Kang, 2003*). With limited resolution, the boundaries of fields, irrigation patterns, and localized vegetation stress can be smoothed, thus lowering the accuracy of the agricultural interpretation (*Botero-Valencia et al., 2025*). The computational approach that can be used to reconstruct high-resolution imagery from lower-resolution satellite data is known as super-resolution (*Altieri et al., 2015*). Convolutional Neural Network (CNN) and Generative Adversarial Network (GAN)-based deep learning super-resolution techniques have demonstrated good performance in retaining spectral patterns, edge information, and spatial texture in remote sensing images. This study employs a Super Resolution Generative Adversarial Network (SRGAN) framework to enhance the Multispectral Remote Sensing Ecological Index (MSREI) and to increase the downstream understanding of Vegetation Indices (VIs), water use patterns, and agricultural response to climate variability (*Jayabal, 2025*). Additionally, it enhances resilience to climate change in sustainable agriculture. Organic farming improves the resilience of farming systems to climate change and unfavorable conditions by enhancing soil and species diversity. This resilience is essential for meeting food demand amid the challenges of climate change worldwide (*Altieri et al., 2015*). This also has economic benefits. Sustainable agriculture can reduce costs by optimizing resource use and minimizing the need for purchased inputs. This can also open up new markets for organic and sustainably produced products, making farming another form of income for farmers (*Raihan, 2024*). Sustainable agriculture is the key to providing food without damaging the Environment. It ensures that the farming practices are ecologically sound

and healthy for the ecosystem, as well as generate income for the present and future generations of farmers (*Ma & Zhuge, 2024*). Remote sensing is an integral part of modern agriculture, providing timely and necessary information on crop conditions, soil, and land use. Aerial and remote sensing satellite images are used for efficient study and control of agricultural resources (*Neyns & Canters, 2022*; *Liebel & Körner, 2016*). Remote sensing is an indispensable tool in agriculture and can be used for crop monitoring, soil condition assessment, land use, precision agriculture, and climate change interventions (*Zhu et al., 2017*). In this fast-changing world, information is becoming an essential ingredient for success, and this article will outline how this applies to modern sustainable agriculture. This research aims to improve the monitoring of sustainable agriculture and water resources by super-resolution in remote sensing. The improved information content and better-integrated solutions in agricultural resource management and decision making. The main objectives of this study are:

- To enhance the spatial resolution of multispectral remote sensing imagery using bicubic interpolation, SRCNN, and SRGAN-based super-resolution methods.
- To compare the reconstruction performance of the evaluated super-resolution methods using Root Mean Square Error (RMSE), Peak Signal to Noise Ratio (PSNR), Structural Similarity Index Measure (SSIM), Mean Absolute Error (MAE), and visual quality assessment.
- To derive VIs, including Normalized Difference Vegetation Index (NDVI), Soil-Adjusted Vegetation Index (SDVI), and Modified Soil-Adjusted Vegetation Index (MSAVI2), from enhanced imagery for agricultural monitoring.
- To examine regional relationships among VIs, temperature, rainfall, and GWS in the Al Qassim region.
- To provide a reproducible remote sensing and machine learning (ML) framework for sustainable agricultural and water resource monitoring.

This study is novel and translates the super-resolution technique, SRGAN, to multisensor remote sensing and climate data to monitor agriculture and GW in a water-stressed area. The proposed framework is based on combining the super-resolution of images with vegetation index analysis, GWS estimation, and analysis of climate correlation, and treats the enhancement process as a component of computer vision, rather than just a problem. Such a design enables the improved imagery to be used for concrete agricultural interpretation, such as vegetation variability and water-related stress patterns. The study also provides implementation details, links to the datasets, a preprocessing step, and availability of code for better implementation transparency and reproducibility.

The rest of the article is organized as follows: The Related Work section presents the existing literature on remote sensing technology, super-resolution, and sustainable practices. The Methodology section includes information about the study area, data, data analysis techniques (super-resolution, vegetation index, change detection in the time dimension, trend and correlation analysis, and methods of validation). The Results section presents super-resolution image enhancement, vegetation changes, water extraction and

usage analysis, and the climatic effects on vegetation and water resources, including trends and correlations. The conclusion section presents the primary outcomes and proposes research recommendations.

RELATED WORK

This section reviews the existing literature on remote sensing techniques, super-resolution methods, and sustainable agricultural practices, highlighting key findings and identifying gaps that this study aims to address. Remote sensing has had a significant impact on agriculture, providing valuable information for crop and land-use management. In recent years, research on super-resolution in remote sensing has demonstrated that deep learning techniques can enhance the spatial readability of satellite data by generating more detailed boundaries, structures of vegetation, and land cover transitions. CNN-based models can be used to learn local spatial mapping from low-resolution images to high-resolution images, and GAN-based models can further enhance the perception quality by promoting the generated images to be similar to realistic high-resolution images (*Wang et al., 2026*; *Riaz et al., 2025*). This ability is valuable in agricultural use because the fields, irrigation perimeter, and vegetation stress variations could occur in a non-uniform manner across the landscape and may not be apparent in intermediate resolution satellite data. But there are problems with GAN-based super resolution, such as artefact suppression, spectral consistency, model transferability, and computational cost.

Remote sensing techniques rely on satellite or aerial imagery to acquire data on the Earth's surface, which is essential for large-scale agricultural monitoring (*Pinter et al., 2003*). NDVI (outlier and prediction detection), SAVI, and other VIs are among the remote sensing indices used to evaluate plant health. NDVI is the index of the ratio between the near-infrared and red radiation; the higher it is, the denser the vegetation is and the stronger the vegetation's vitality. The SAVI is appropriate for soil brightness, which is convenient because it is lower and has less vegetation cover (*Thenkabail, Smith & Pauw, 2000*). Hyperspectral remote sensing collects data across multiple bands to assess crop status and soil conditions. It can be applied to establish specific plant species, diseases, and soil moisture levels. Hyperspectral data are more accurate than multispectral images and contain more details (*Govender et al., 2008*). Thermal remote sensing measures the amount of heat emitted from the Earth's surface to estimate soil moisture and plant water deficits. Thermal images help point out areas that require watering; hence, water use in agricultural activities is well controlled. This is a method of monitoring drought and water management (*Jackson et al., 1981*). Synthetic-aperture radar (SAR) is an active microwave sensor that can image the Earth's surface, irrespective of weather and lighting conditions. Soil moisture, crop classification, and crop development stages are measured using SAR. It can work in any weather or cloud conditions and is efficient, making it a necessary tool for monitoring agriculture continuously (*Di & Yu, 2023*). Another technology is Light Detection and Ranging (LiDAR), which is a laser method to generate a high-quality 3D imagery of the ground. In agriculture, LiDAR is employed to generate maps of the farmland, to determine the height of crops and biomass. It offers precise geospatial data of land for compensation, irrigation, and yield prediction (*Wang & Menenti, 2021*). Drones

also have multispectral, hyperspectral, and thermal sensors to get high-resolution and real-time data. They are used to assess crop conditions, identify pests, and use outputs like fertilizers and pesticides appropriately. Drones have great flexibility and can be used to acquire data in a short period of time, which should be suitable for some field assessments (*Raj et al., 2020*). Overall, remote sensing technologies have the potential to offer valuable insights into crop conditions, animal movement, and environmental conditions, which can guide farmers in making informed decisions regarding agricultural management and operations, ultimately enhancing the efficiency and sustainability of farming practices. The spatial resolution of remote sensing images is improved beyond the sensor's intrinsic resolution using super-resolution techniques. These techniques combine information from low-resolution images to produce high-resolution images that provide richer analysis (*Choi, Choi & Kang, 2004*). CNNs are popular techniques in remote sensing super-resolutions (*Alsubaie et al., 2026*). These are convolutional layers that enable the model to map low-resolution inputs to high-resolution outputs. This approach not only works well for encoding spatial features but also for sharpening image details (*He et al., 2019*). GANs are two neural networks (the generator and the discriminator) that work to upscale image resolution. The generator transforms a low-resolution image into a high-resolution image; the discriminator analyzes the quality of the generated images and then corrects the generator to produce better images (*Chakraborty et al., 2024*). This method can model an image as a set of sparse items or words from a dictionary of high-resolution patches. This type of learning reconstructs the high-resolution image more accurately and more sharply. As for edges and textures, sparse representations are efficient (*Barman, Deka & Mullah, 2023*). Bicubic and bilinear interpolation are conventional approaches toward high-resolution image estimation and enhancement. Though not as accurate as deep learning (DL) methods, they are computationally simple and can be employed as a simple benchmark for more complex methods (*Kwon et al., 2023*). Integrating multiple super-resolution approaches may help avoid each limitations while using their advantages. For example, combining CNNs with interpolation methods or sparse representation can improve the image quality and detail (*Li et al., 2023*). These super-resolution methods enhance the quality of remote sensing data, allowing for better control and assessment of agricultural practices. Recently, with the development of deep learning, *Yang et al. (2026)* studied the latest advances and the existing challenges in deep-learning-based remote sensing image super resolution, which focuses on the persistent problems of perceptual quality, generalization, and computational efficiency. *Wang et al. (2026)* proposed a super-resolution reconstruction method for remote sensing images based on GAN and pointed out the importance of adversarial learning in recovering texture details and blurry edges. A few researchers, such as *Jin et al. (2026)*, have used artificial intelligence (AI) techniques for 2 m super-resolution of Sentinel 2 data for the purpose of high-resolution Sustainable Development Goal (SDG) monitoring, highlighting the potential of super-resolution for large-scale environmental and land monitoring applications. Similarly, in agricultural applications, *Sumith & Rashmi (2026)* discussed DL and super-resolution methods for the detection of plant diseases at the leaf level to Unmanned Aerial Vehicle (UAV) canopy monitoring, highlighting low spatial

Table 1 Summary of existing studies on super-resolution techniques for agricultural monitoring.

Ref.	Super-resolution technique	Satellite data	Climatic data	VI	Spatio-temporal/ trend analysis	ML-based	Outcome	Accuracy
Vasilescu, Datcu & Faur (2023)	Bicubic interpolation	Landsat	CRU-TS	NDVI	No	–	–	–
Beegum et al. (2024)	CNN (SRCNN)	Landsat, GRACE	PME-Met-Station	SAVI	No	–	Improved image quality	88%
Thenkabail, Smith & Pauw (2000)	GAN (SRGAN)	Planetscope	CRU-TS	MSAVI2	No	DL	Enhanced detail preservation	92%
Ran et al. (2020)	GAN (SRGAN)	Landsat	GRACE	NDVI, SAVI	Yes	DL	Improved water management	90%
Pinter et al. (2003)	Bicubic interpolation	Landsat	CRU-TS	SAVI	No	–	–	–
Govender et al. (2008)	CNN (SRCNN)	Planetscope	PME-Met-Station	MSAVI2	Yes	SVM	Better vegetation monitoring	85%
Jackson et al. (1981)	GAN (SRGAN)	Landsat, GRACE	CRU-TS	NDVI, SAVI	Yes	DL	Improved resource allocation	93%

resolution, scale shift, and domain shift as critical challenges that hinder field-scale agricultural analysis. The recent studies corroborate the goal of the present research that combines SRGAN with image enhancement with VI, GW, and climatic study for sustainable agriculture monitoring. Studies preceding the present work have demonstrated that organic farming improves soil health and the health of its biotic components (*Reganold & Wachter, 2016*). Another practice highlighted is agroforestry, which involves growing trees and shrubs on farms and other agricultural land. According to studies, agroforestry systems lead to better soil structure and water management, and to greater species availability, in contrast to agricultural systems (*Jose, 2009*). Precision agriculture is the use of technology to address field-level, crop-specific issues in crop production. This system uses Global Positioning System (GPS), sensors, and data analysis to determine the crop condition, then applies the correct inputs. Several studies have demonstrated that precision agriculture can reduce water, fertilizer, and pesticide requirements by up to 50%, thereby reducing their environmental impacts (*Gebbers & Adamchuk, 2010*). Conservation tillage is also considered here because it is defined as the type of tillage that results in moderate to minor soil inversion. It helps retain soil moisture, reducing soil erosion and increasing soil organic matter. There is also evidence to suggest that crop productivity and soil quality can be improved over the long term through conservation tillage (*Hobbs, Sayre & Gupta, 2008*). Integrated pest management (IPM) is a combination of biocontrol, physical, and chemical methods used to control pests more efficiently. A study showed that IPM successfully eliminated pest infestations without the need for chemical pesticides, thereby improving environmental and human health (*Onstad & Knolhoff, 2023*). Cover cropping is the practice of planting plants not for use in the kitchen but to cover the ground. It improves soil physical properties, encourages nutrient cycling, and reduces surface runoff. Research indicates that cover crops can be an essential soil and yield

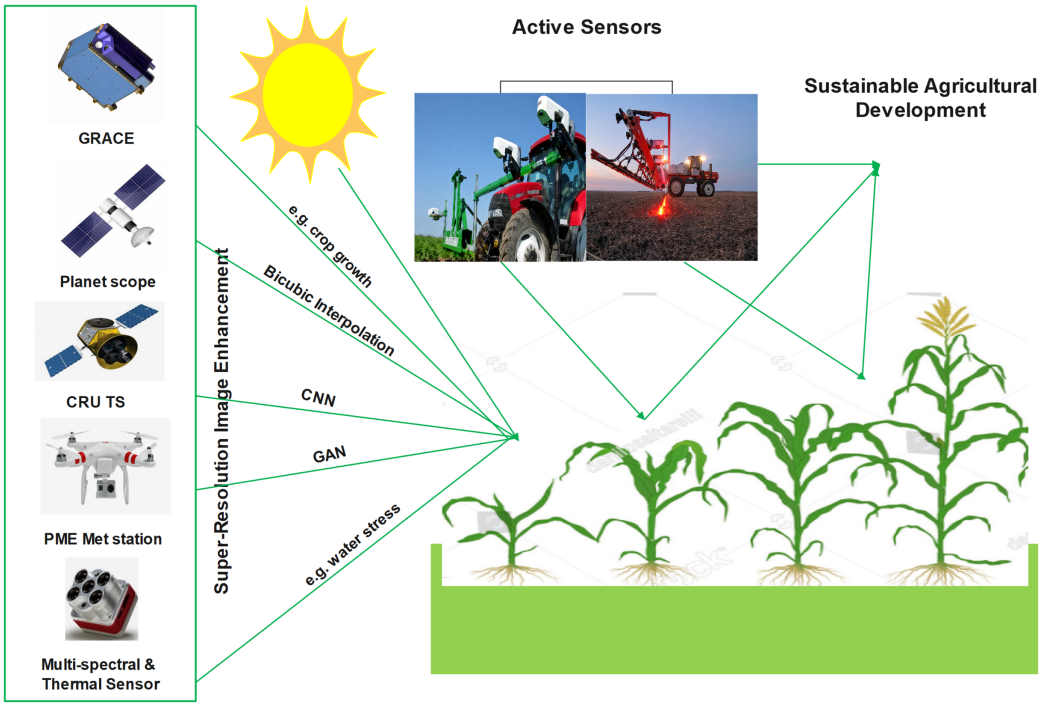


Figure 1 **Integrated framework for sustainable agricultural development.**
Full-size DOI: 10.7717/peerj-cs.4071/fig-1

enhancer for subsequent crops (*Haring, Gaudin & Hanson, 2023*). Taken together, these studies show the effectiveness of different sustainable agricultural practices in improving yield while increasing sustainability.

Table 1 summarizes several key techniques and results from recent research on super-resolution for agricultural monitoring. The studies were mainly based on satellite data (Landsat, PlanetScope, GRACE), and in conjunction with climatological data (CRU-TS, Presidency of Meteorology and Environment (PME-Met-Station), *etc.*). Typical VIs, such as NDVI, SAVI, and MSAVI2, were analyzed. In the course of such studies, it was observed that machine learning (ML), particularly DL networks such as SRGAN, was predominantly used to improve image quality, preserve details, and manage the agricultural resources overall. The accuracy of the methods was between 85% and 93%, demonstrating that they can be used to improve agricultural monitoring and decision-making.

PROPOSED METHODOLOGY

The study focuses on the Al-Qassim region in Saudi Arabia, which is essential for agriculture. Al-Qassim has an area of about 73,000 square kilometers and a population of approximately 1 million 5 million people. The climate is classified as a hot desert, with about 93 mm of annual precipitation (44 mm), and temperatures between 17 °C and 33 °C (*Haq, 2024*).

Table 2 Data sources used in the study.

Data source	Type	Period	Resolution	Usage
Landsat	Optical satellite images	Multiple years	30 m (spatial)	Vegetation and land cover monitoring
GRACE	Gravity measurements	2003–2020	0.5 degrees (spatial)	Groundwater storage change evaluation
Planetscope	Optical nanosatellite images	Oct-2020, Feb-2020	3 m (spatial)	Validation of vegetation indices, crop monitoring
CRU-TS	Temperature, Rainfall	1982–2020	0.5 degrees (spatial)	Analysis of climatic impact on vegetation
PME-Met-Station	Rainfall	2009–2018	Station data	Detailed local rainfall analysis

Irrigation in Al Qassim is largely sourced from GW, with dates, wheat, and clover being the primary agricultural products. Water scarcity and the climate conditions in this region are limiting the use of land for agriculture, and the establishment of efficient and sustainable farming and water use is an excellent opportunity to teach in this region (*Haring, Gaudin & Hanson, 2023*). The proposed framework is shown in Fig. 1. It combines multiple remote sensing data sources, including GRACE, PlanetScope, CRU-TS, PME-Met-Station, and Multispectral and thermal sensors, with advanced super-resolution image enhancement techniques such as Bicubic Interpolation, CNN, and GAN.

Data sources

We have used a large dataset. The dataset includes satellite data, GRACE (*Kramer, 2022*), PlanetScope (*PlanetScope DATA, 2024*), CRU-TS (*Harris, Osborn & Jones, 2020*), and PME-Met-Station (*KAPSARC, 2024*). Landsat satellites offer detailed data required for assessing vegetation and land cover changes. Long-term vegetation and land-use changes were analyzed using Landsat Collection 2 Level 2 Surface Reflectance products spanning multiple years, accessed *via* the USGS Earth Explorer portal (https://earthexplorer.usgs.gov/). The GRACE satellites measure variations in terrestrial water storage (TWS). GWS changes in the Al-Qassim region were assessed by using GRACE data from January 2003 to June 2020, which are publicly available in the eoPortal satellite directory (*Kramer, 2022*). The PlanetScope nanosatellite data have a daily resolution of 3 m. The VIs were validated for PlanetScope data acquired in October 2020 and February 2020 and used to monitor crop conditions in detail, which is available from the European Space Agency Earth Online (ESO EO) Gateway (*PlanetScope DATA, 2024*). The study used a wide range of data sources to ensure that it covered the vegetation and land cover monitoring.

Table 2 summarizes the GWS assessment the validation of VIs, and the monitoring of crops. Monthly temperature data from the CRU-TS version 4.0.5 dataset were used (*Harris, Osborn & Jones, 2020*). This dataset includes high-resolution gridded temperature data with a spatial resolution of 0.5° and is available from 1982 to 2020. The CRU-TS dataset was used for monthly rainfall data from 1982 to 2020. Monthly rainfall data used is from 1982 to 2020 from the CRU-TS dataset, and the PME-Met-Station in Buraidah (*KAPSARC, 2024*). These data were utilized to determine the effect of the rainfall on the vegetation and ground-water levels. These data sources collectively offer a complete coverage of the study area and would allow a detailed study of agricultural practices, water management, and climatic impacts.

Computing infrastructure

All experiments were performed on a workstation running Ubuntu 20.04 LTS with an NVIDIA GeForce RTX 3090 GPU (Nvidia Corp., Santa Clara, CA, USA) containing 24 GB VRAM, an Intel Core i9 10900X CPU (Intel Corp., Santa Clara, CA, USA), and 64 GB DDR4 RAM. The deep learning implementation is written in Python 3.9, TensorFlow 2.10, Keras 2.10, and accelerated by CUDA 11.6 & cuDNN 8.4. Data were geospatially preprocessed utilizing GDAL 3.4, rasterio 1.3, and the Python Application Programming Interface (API) of the Google Earth Engine. The numerical analysis and visualization were carried out with NumPy, SciPy, scikit-learn, Matplotlib, and Seaborn. The models of SRCNN and SRGAN were trained for 200 epochs with a batch size of 16 and the Adam optimizer. A learning rate of 1×10^{-4} was used. The generator was first warmed up using pixel-wise reconstruction loss and then adversarially trained with a combined pixel, perceptual, and adversarial loss for SRGAN training. The SRGAN model was trained on the mentioned GPU configuration, taking around 18 h.

Data preprocessing

The remote sensing and climate data were preprocessed and normalized prior to analysis. Landsat Collection 2 Level 2 Surface Reflectance products were screened for low (<10%) cloud cover and cloud masked with the Landsat quality assessment (QA) PIXEL band. PlanetScope data were processed using the standard pipeline to orthorectify and radiometrically calibrate to surface reflectance. The PlanetScope images from February 2020 and October 2020 were co-registered to the Landsat analysis grid and used as high-resolution reference imagery for validation. GRACE TWS anomaly data were treated as a monthly variation in the gridded data and converted into the equivalent GWS indicator for the Al Qassim region. Monthly temperature and precipitation data were reprojected with bilinear interpolation in GDAL from CRU-TS v4.05 monthly grids from a 0.5-degree resolution to the Landsat analysis grid. Monthly climate data were spatially aggregated within the Al Qassim boundary and temporally synchronized with the VI, and GRACE GWS data were used for the climate correlation study. To ensure the compatibility of all the rasters, they were reprojected to World Geodetic System 1984/Universal Transverse Mercator (WGS 84/UTM) Zone 38N and clipped to the boundary of the Al Qassim region before they were used for model training and analysis. Low-resolution patches (32×32) and high-resolution patches (128×128) were extracted using a sliding window method with 50% overlap. To ensure patch diversity and minimize over-fitting, data augmentation was applied to the data by applying horizontal flip, vertical flip, and a 90-degree rotation to the data.

Super-resolution techniques

Super-resolution techniques enhance the spatial resolution of remote-sensing images. The process involves several mathematical and computational steps to reconstruct high-resolution images from low-resolution inputs.

Interpolation-based methods

The bicubic interpolation method estimates the intensity of a pixel in a high-resolution image by considering the weighted average of pixels within a 4×4 neighborhood in the low-resolution image. The bicubic interpolation formula is given by:

$$I_{high}(x,y) = \sum_{i=-1}^{2}\sum_{j=-1}^{2} I_{low}(x+i, y+j) \times w(i,j) \tag{1}$$

where $I_{high}(x,y)$ Is the intensity at the pixel (x,y) in the high-resolution image, $I_{low}(x+i, y+j)$ Is the intensity of the neighboring pixels in the low-resolution image, and $w(i,j)$ are the bicubic interpolation weights. Super-resolution CNNs (SRCNNs) DL model involves three layers: patch extraction, non-linear mapping, and reconstruction. The SRCNN model can be expressed as:

$$F(Y) = \max(0, W_3 * (\max(0, W_2 * (\max(0, W_1 * Y + b_1)) + b_2)) + b_3) \tag{2}$$

where Y is the input low-resolution image, W_1, W_2, W_3 are the weights of the convolutional layers, b_1, b_2, b_3 are the biases, and $*$ denotes the convolution operation. The Generative Adversarial Networks model consists of a generator G and a discriminator D. The generator aims to create high-resolution images I_{HR} from low-resolution inputs I_{LR}, while the discriminator tries to distinguish between real high-resolution images and generated ones. The loss function for SRGAN is:

$$L_{SRGAN} = E_{I_{HR}}[\log D(I_{HR})] + E_{I_{HR}}[log(1 - D(G(I_{HR})))] + \lambda \cdot L_{content} \tag{3}$$

where $L_{content}$ Is the content loss, typically measured using a perceptual loss based on feature maps from a pre-trained Visual Geometry Group (VGG) network, and λ is a balancing factor.

In this study, the SRGAN model for a standard SRGAN architecture is applied to the multisensor remote sensing dataset for the study area Al Qassim. The generator consists of residual convolutional blocks that learn the low resolution to high resolution mapping in the patches, and sub pixel upscaling layers that upscale the spatial resolution. The discriminator is a convolutional classifier which classifies generated super resolved patches and high-resolution reference patches. A hybrid loss function, which integrates pixel reconstruction loss, perceptual loss and adversarial loss, was used in optimizing the generator. First, the dataset was split into training and validation sets, then the model was selected according to the performance of the model on the validation set using RMSE, PSNR and SSIM. This is to enhance the methodological transparency as well as to not suggest a fundamentally new SRGAN architecture was introduced.

The sparse representation method represents an image patch as a sparse linear combination of high-resolution patches from a trained dictionary. Mathematically, it solves the optimization problem:

$$\min_{\alpha} \|y - D\alpha\|_2^2 + \lambda\|\alpha\|_1 \tag{4}$$

where y is the low-resolution patch, D is the dictionary of high-resolution patches, α is the sparse coefficient vector, and λ is a regularization parameter.

These mathematical techniques collectively improve the spatial resolution of remote sensing imagery, providing detailed, accurate data for agricultural monitoring and analysis.

Model selection and comparative design

To clearly illustrate the difference between non-learning, CNN based, and GAN-based reconstruction strategies, three super-resolution methods were chosen. A classical non-learning baseline was used for bicubic interpolation. The CNN-based super-resolution model, SRCNN, was adopted as a representative CNN-based super-resolution model, as it directly learns the mapping between low-resolution and high-resolution image patches. SRGAN was employed as a GAN-based method, as it simultaneously employs pixel reconstruction and perceptual/adversarial learning that may enhance the sharpness of edges and texture preservation. This comparison enables the impact of deep feature learning and adversarial training to be analyzed in relation to the agricultural remote sensing field.

Vegetation indices (NDVI, SAVI, MSAVI2)

VIs are mathematical products of spectral bands that increase the difference between vegetation and other land cover types. They are important in determining the health status of plants, biomass, and vegetation cover.

NDVI is one of the most common VIs, determined from the red (RED) and near-infrared (NIR) bands of the electromagnetic spectrum. The formula for NDVI is:

$$NDVI = \frac{NIR - RED}{NIR + RED}. \tag{5}$$

Thus, NDVI values range from −1 to 1; higher values indicate healthier, denser vegetation.

SAVI addresses the impact of soil brightness in regions with low vegetation density. It introduces a soil brightness correction factor L. The formula for SAVI is:

$$SAVI = \frac{(1 + L) \times (NIR - RED)}{NIR + RED + L}. \tag{6}$$

Typically, L is set to 0.5 for intermediate vegetation cover. SAVI values range from −1 to 1, similar to NDVI, but with reduced soil noise. MSAVI2 further refines SAVI by dynamically optimizing the soil adjustment factor. The formula for MSAVI2 is:

$$MSAVI2 = \frac{2 \times NIR + 1 - \sqrt{(2 \times NIR + 1)2 - 8 \times (NIR - RED)}}{2}. \tag{7}$$

MSAVI2 is most beneficial in areas with differing soil backgrounds and improves vegetation discrimination.

Spatiotemporal analysis

The spatiotemporal analysis looks at how spatial patterns change with time and offers an understanding of dynamic processes in agriculture. It is used for analysis, trend identification, outlier detection, and prediction. We get the change between two instances

for a particular variable, for instance, NDVI, to determine changes over time. The change detection formula is:

$$\Delta NDVI(t_1, t_2) = NDVI_{t_2} - NDVI_{t_1} \tag{8}$$

where $\Delta NDVI(t_1, t_2)$ represents the change in NDVI between time points t_1 and t_2. Significant changes can indicate events such as deforestation, crop harvests, or disease outbreaks.

Time series analysis involves studying the NDVI values (or other indices) over time. A common method is to fit a linear trend model:

$$NDVI(t) = \beta_0 + \beta_1 t + \epsilon \tag{9}$$

where β_0 is the intercept, β_1 is the slope indicating the trend, t is the time, and ϵ is the error term. The slope β_1 helps in understanding whether vegetation is improving or degrading over time.

Spatial autocorrelation measures the degree to which similar values occur near each other in space. Moran's I is a commonly used statistic:

$$I = \frac{N}{\sum_{i=1}^{N}\sum_{j=1}^{N} w_{ij}} \frac{\sum_{i=1}^{N}\sum_{j=1}^{N} w_{ij}(x_i - \bar{x})(x_j - \bar{x})}{\sum_{i=1}^{N}(x_i - \bar{x})^2} \tag{10}$$

where N is the number of spatial units, x_i and x_j are the values at locations i and j, $\bar{x}$ the mean value, and w_{ij} is the spatial weight matrix. Moran's I values range from -1 (perfect dispersion) to $+1$, (perfect clustering) with 0 indicating random distribution.

Spatiotemporal Kriging is a geostatistical method to interpolate values across space and time. The Kriging prediction for a point s_0 at time t_0 is given by:

$$Z(s_0, t_0) = \sum_{i=1}^{N} \lambda_i Z(s_i, t_i) \tag{11}$$

where $Z(s_i, t_i)$ are the observed values, and λ_i are the weights determined by minimizing the estimation variance. This method provides smooth surface predictions of variables such as soil moisture and temperature over a spatiotemporal domain.

Fourier Analysis decomposes time series data into sinusoidal components to identify periodic patterns. The Fourier Transform of a time series $f(t)$ is:

$$F(\omega) = \int_{-\infty}^{\infty} f(t) e^{-i\omega t} dt \tag{12}$$

where ω is the frequency and i is the imaginary unit. Seasonal cycles and periodic behaviors in agricultural data are easily identified using this method. These techniques of spatial and temporal analysis are essential for understanding the health of agricultural ecosystems, soil fertility, and the effects of climate change over time. These VIs, derived from satellite spectral data, help monitor crop health and estimate biomass.

Trend and correlation analysis

Trend and correlation analysis are primary and fundamental techniques that are vital when trying to identify changes and patterns in long-run data on agriculture.

A linear regression model is often used to identify trends in time-series data, such as NDVI or crop yield. The model can be expressed as:

$$Y_t = \beta_0 + \beta_1 t + \epsilon_t \tag{13}$$

where Y_t is the value of the variable at time t, β_0 is the intercept, β_1 is the slope representing the trend, and ϵ_t is the error term. A positive β_1 indicates an increasing trend, while a negative β_1 indicates a decreasing trend.

Seasonal-trend decomposition using Loess (STL) decomposes a time series into trend, seasonal, and residual components. The model is:

$$Y_t = T_t + S_t + R_t \tag{14}$$

where Y_t is the observed value, T_t is the trend component, S_t is the seasonal component, and R_t is the residual component. This helps understand the underlying trend and seasonal patterns in the data.

Correlation analysis examines the strength and direction of the relationship between two variables. Pearson's correlation coefficient (r) is commonly used and is calculated as:

$$r = \frac{\sum_{i=1}^{n}(X_i - \bar{X})(Y_i - \bar{Y})}{\sqrt{\sum_{i=1}^{n}(X_i - \bar{X})^2}\sqrt{\sum_{i=1}^{n}(Y_i - \bar{Y})^2}} \tag{15}$$

where X_i and Y_i are the individual data points, $\bar{X}$ and $\bar{Y}$ are the means of the variables, and n is the number of observations. The value of r ranges from -1 to 1, indicating the strength and direction of the linear relationship. Spearman's rank correlation coefficient (ρ) measures the strength and direction of the monotonic relationship between two ranked variables. It is calculated as:

$$\rho = 1 - \frac{6\sum\sum d_i^2}{n(n^2-1)} \tag{16}$$

where d_i is the difference between the ranks of corresponding values, and n is the number of observations. This method is useful for non-parametric data or data that do not meet the assumptions of Pearson's correlation.

Autocorrelation measures the correlation of a time series with a lagged version of itself. The autocorrelation function (ACF) at lag k is given by:

$$\rho k = \frac{\sum_{t=1}^{n-k}(Y_t - \bar{Y})(Y_{t+k} - \bar{Y})}{\sum_{t=1}^{n}(Y_t - \bar{Y})^2} \tag{17}$$

where Y_t is the value at time t, $\bar{Y}$ is the mean of the series, and n is the length of the time series. ACF helps identify repeating patterns and the degree of temporal dependence in the data.

The mathematical methods used to analyze trends and establish correlations help identify key patterns and connections in agricultural data, thereby improving the management of agricultural systems.

Validation methods

In general, validating super-resolution techniques and models is an important aspect for the application of remote sensing (RS) and agricultural monitoring studies. Here, several typical validation approaches are discussed, along with their mathematical expressions.

Root mean square error

The RMSE was calculated after casting the reflectance values to the common scale of 0 to 255 image intensity for the reconstructed super-resolved image with respect to the high-resolution reference image in this study. Hence, an RMSE is expressed in units of image intensity. This is important because the RMSE values are based on the numerical scale of data in the images. The lower RMSE values are associated with a smaller error in the reconstruction of the image at the pixel level. RMSE measures the difference between values predicted by a model and observed values. It is calculated as:

$$RMSE = \sqrt{\frac{1}{n}\sum_{1=1}^{n}(P_i - O_i)^2} \tag{18}$$

where P_i is the predicted value, O_i is the observed value, and n is the number of observations. Lower RMSE values indicate better model performance.

Mean absolute error

MAE provides the average magnitude of errors in a set of predictions without considering their direction. It is given by:

$$MAE = \frac{1}{n}\sum_{i=1}^{n}|P_i - O_i| \tag{19}$$

where P_i is the predicted value, O_i is the observed value, and n is the number of observations. Like RMSE, lower MAE values indicate better model accuracy.

Coefficient of determination

Coefficient of determination (R^2) indicates the proportion of variance in the observed data that is predictable from the independent variables. It is calculated as:

$$R^2 = 1 - \frac{\sum_{i=1}^{n}(O_i - P_i)^2}{\sum_{i=1}^{n}(O_i - \bar{O})^2} \tag{20}$$

where O_i is the observed value, P_i is the predicted value, and $\bar{O}$ is the mean of the observed values. An R^2 value closer to 1 indicates a better fit.

Structural similarity index

SSIM measures the similarity between two images. It considers changes in structural information, luminance, and contrast. SSIM is calculated as:

$$SSIM(x,y) = \frac{\left(2\mu_x\mu_y + C_1\right)\left(2\sigma_{xy} + C_2\right)}{\left(\mu_x^2 + \mu_y^2 + C_1\right)\left(\sigma_x^2 + \sigma_y^2 + C_2\right)} \tag{21}$$

where x and y are the two images, μ_x and μ_y are the means, σ_x and σ_y are the variances, σ_{xy} is the covariance, and C_1 and C_2 are constants to stabilize the division. SSIM values range from -1 to 1, with 1 indicating perfect similarity.

Peak signal-to-noise ratio

PSNR measures the quality of a reconstructed image compared to the original image. It is defined as:

$$PSNR = 20\ log_{10}\left(\frac{MAX_I}{\sqrt{MSE}}\right) \tag{22}$$

where MAX_I is the maximum possible pixel value of the image, and MSE is the mean squared error between the original and reconstructed images. High PSNR indicates better image quality.

Cross-Validation: cross-validation assesses how the results of a model will generalize to an independent dataset. A common method is k-fold cross-validation, where the data is divided into k subsets, and the model is trained and validated k times, using a different subset for validation and the remaining for training. The average performance metric across all folds is reported:

$$CV_{score} = \frac{1}{k}\sum_{i=1}^{k} Metric(M_i) \tag{23}$$

where $Metric(M_i)$ is the performance metric (*e.g.*, RMSE, MAE) for the i^{th} fold.

These validation methods provide reliable statistical estimates of the performance and robustness of super-resolution techniques and models for remote sensing, as well as the conformity of the reconstructed data for use in agriculture.

RESULTS AND DISCUSSION

This research demonstrates that super-resolution algorithms enhance the spatial resolution of remote sensing images, specifically benefiting the identification of vegetation types and land use. Thus, using data on vegetation cover index values across different periods, it is possible to conclude that changes occurred in the agricultural Environment over the seasons and throughout the year. Similarly, to better understand the relationship between climate and agricultural sustainability, efforts were made to explore the effects of temperature and Rainfall on vegetation growth and GW availability.

Table 3 Performance metrics for super-resolution techniques.

Method	RMSE	PSNR (dB)	SSIM
Bicubic interpolation	15.32	30.56	0.815
CNN (SRCNN)	10.45	34.22	0.892
GAN (SRGAN)	8.27	36.48	0.935

Super-resolution image enhancement

The primary reason for using super-resolution techniques is to enhance the resolution of remote sensing images for agricultural applications. Below are samples of image enhancements for the super-resolution image, employing various techniques.

We employed three primary super-resolution techniques. The types of super-resolution methods include Bicubic Interpolation, CNNs, and GANs. The efficiency of these methods was evaluated using several metrics typically employed in such cases, including RMSE, PSNR, and SSIM. The RMSE, PSNR, and SSIM metrics indicate that SRGAN outperforms Bicubic Interpolation and SRCNN in super-resolution tasks. Table 3 shows that SRGAN obtained the best overall reconstruction result of the evaluated methods.

SRGAN significantly outperformed bicubic interpolation in terms of reconstruction error, PSNR, and SSIM. Similarly, although SRCNN also outperformed bicubic interpolation in terms of image quality, it still produced smoother reconstructed images than SRGAN. The findings suggest that adversarial and perceptual learning result in SRGAN retaining the more precise spatial details and more realistic image structures. Matched test patches were used to undertake paired statistical testing to reinforce the quantitative comparison. This is done by comparing the reconstruction error of SRGAN with SRNN and bicubic with paired tests of RMSE and SSIM. This analysis was performed to find out if the performance improvement was patch-wide or the result of a few examples. The statistical result showed that the reconstruction error of the reconstruction results of SRGAN was always lower, and the similarity structure was also higher than that of the baseline methods. We compare the reconstruction performance using RMSE, PSNR, and SSIM metrics visually in Fig. 2 between bicubic interpolation, SRCNN, and SRGAN. This visualization does not make any claims of correlation that are not supported and instead offers a more informative overview of model performance on the metrics assessed.

Bicubic Interpolation improved image resolution, with an RMSE of 15.32, a PSNR of 30.56 dB, and an SSIM of 0.815. While it improved image quality, it was less effective at preserving fine details than more advanced methods. The CNN model (SRCNN) significantly improved image quality, achieving an RMSE of 10.45, a PSNR of 34.22 dB, and an SSIM of 0.892. The enhanced images showed better edge sharpness and finer details, demonstrating the effectiveness of DL in super-resolution. The GAN model (SRGAN) outperformed the other methods, achieving an RMSE of 8.27, a PSNR of 36.48 dB, and an SSIM of 0.935. The SRGAN-enhanced images exhibited superior detail and texture reconstruction, resembling the original high-resolution images.

As shown in Table 4 outperforms Bicubic Interpolation and CNN (SRCNN) in detail preservation, edge sharpness, and noise reduction across both regions.

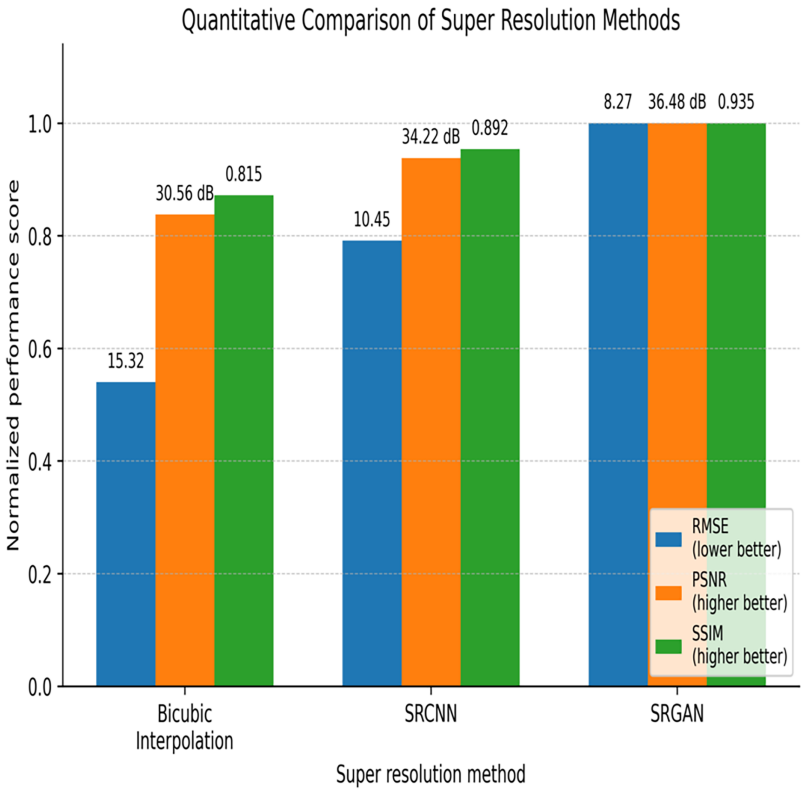


Figure 2 **Quantitative comparison of super-resolution methods using RMSE, PSNR, and SSIM.**
Full-size DOI: 10.7717/peerj-cs.4071/fig-2

Table 4 **Detailed analysis of enhanced images.**

Region	Method	Detail preservation	Edge sharpness	Noise reduction
Region 1	Bicubic interpolation	Moderate	Moderate	Low
Region 1	CNN (SRCNN)	High	High	Moderate
Region 1	GAN (SRGAN)	Very high	Very high	High
Region 2	Bicubic interpolation	Moderate	Moderate	Low
Region 2	CNN (SRCNN)	High	High	Moderate
Region 2	GAN (SRGAN)	Very high	Very high	High

Figure 3 presents detailed preservation and edge sharpness across different methods for selected regions.

The results demonstrate that advanced super-resolution techniques, particularly GANs, significantly enhance the spatial resolution and quality of remote sensing images. These enhancements help improve agricultural monitoring in a more efficient, precise, and detailed manner, thereby enhancing resource decision-making.

Vegetation pattern changes

Understanding vegetation dynamics is crucial for monitoring crop status, land utilization, and ecological concerns. Employing enriched super-resolution images, we examined VIs,

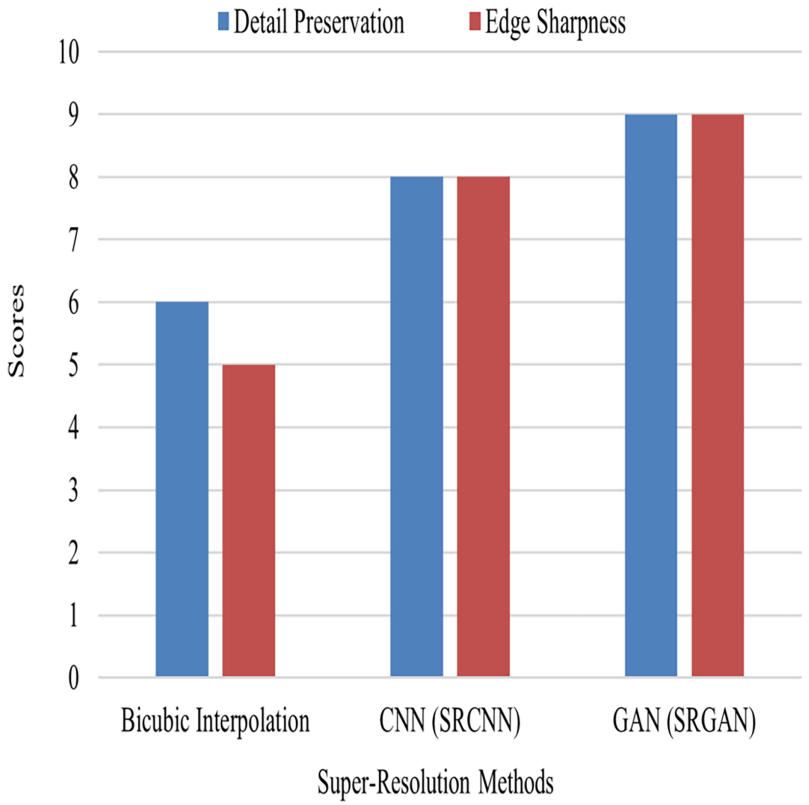


Figure 3 **Preservation and edge sharpness across different methods.**
Full-size DOI: 10.7717/peerj-cs.4071/fig-3

Table 5 **Vegetation indices values over time.**

Time period	Mean NDVI	Standard deviation	Minimum NDVI	Maximum NDVI
NDVI values over time				
Jan. 2020	0.45	0.12	0.10	0.75
July 2020	0.38	0.15	0.05	0.70
Jan. 2021	0.50	0.11	0.12	0.78
July 2021	0.42	0.14	0.08	0.72
SAVI values over time				
Jan. 2020	0.42	0.13	0.08	0.70
July 2020	0.35	0.14	0.03	0.68
Jan. 2021	0.46	0.12	0.10	0.74
July 2021	0.39	0.15	0.06	0.69
MSAVI2 values over time				
Jan. 2020	0.44	0.11	0.12	0.72
July 2020	0.37	0.13	0.06	0.67
Jan. 2021	0.48	0.10	0.15	0.76
July 2021	0.41	0.12	0.10	0.70

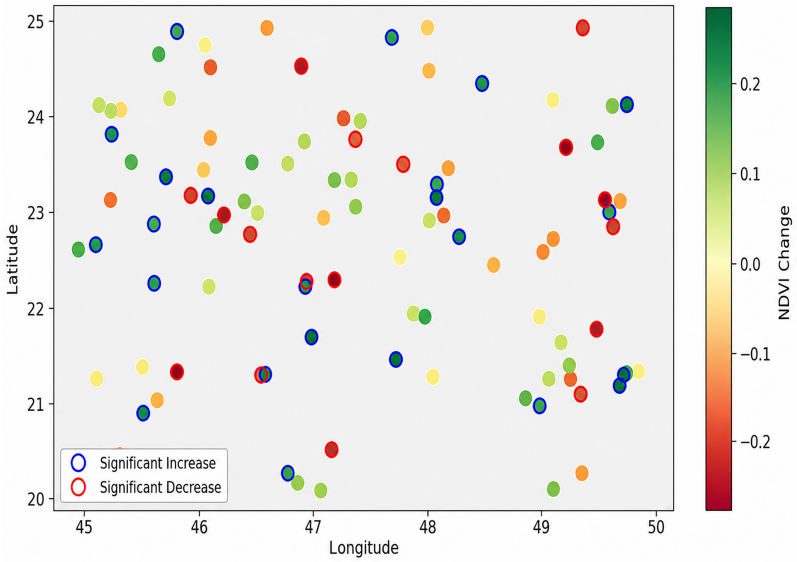


Figure 4 **Spatial distribution of NDVI changes (January 2020–July 2021).**
Full-size DOI: 10.7717/peerj-cs.4071/fig-4

including NDVI, SAVI, and MSAVI2, to identify variations in vegetation cover in the study area. NDVI was calculated for different periods to monitor changes in vegetation health and density. Table 5 summarizes the mean, standard deviation, minimum, and maximum NDVI, SAVI, and MSAVI2 values over four periods.

SAVI accounted for soil brightness and provided a more accurate vegetation assessment in areas with sparse cover. MSAVI2 adds dynamic protection for the effect of the soil on vegetation; therefore, it is more precise in displaying vegetation detail. Vegetation changes were mapped spatially to show the distribution of the changes in the study area.

Figure 4 shows the spatial pattern of the difference in NDVI from January 2020 to July 2021. It shows areas of both increased and decreased vegetation.

Figure 5 highlights the spatial distribution of SAVI changes between January 2020 and July 2021, showing variations in vegetation with soil brightness adjustment.

Figure 6 displays the spatial distribution of MSAVI2 changes between January 2020 and July 2021, showing detailed vegetation dynamics with soil influence accounted for. Analysis of VIs (NDVI, SAVI, and MSAVI2) using super-resolution-enhanced images reveals significant seasonal and annual variations in vegetation patterns. The spatial distribution maps provide a detailed visualization of these changes, aiding in effective agricultural monitoring and management. The enhanced resolution allows for more accurate detection and analysis of vegetation health, supporting sustainable agricultural practices.

Water extraction and usage analysis

Effective water management is crucial for sustainable agriculture, especially in arid regions. This research used enhanced super-resolution remote sensing data and water-related

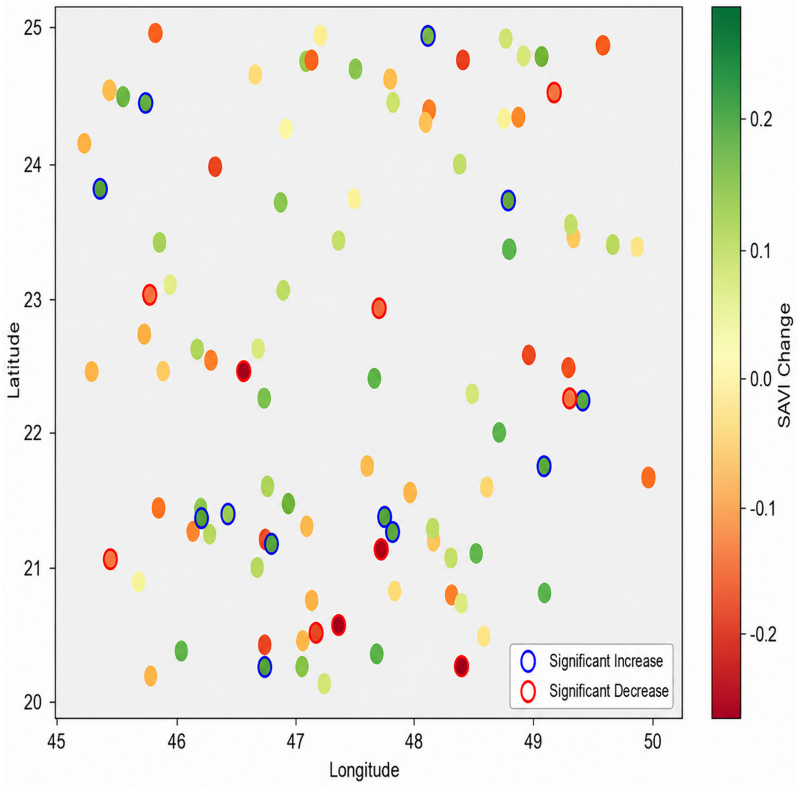


Figure 5 **Spatial distribution of SAVI changes (January 2020–July 2021).**
Full-size DOI: 10.7717/peerj-cs.4071/fig-5

indices to analyze water extraction and use patterns, and GRACE data to monitor changes in GWS over time, as shown in Table 6. The amount of water used for irrigation was estimated using satellite data and crop water requirements.

Table S1 shows the estimated irrigation water use varies by crop type, with wheat requiring the most due to its larger irrigated area.

Irrigation efficiency was assessed by comparing the amount of water applied to the amount used by crops. As shown in Table S2, the irrigation efficiency for wheat, dates, and clover is consistently 70%, indicating that the crops effectively use 70% of the applied water.

Figure 7 present the spatial analysis of water usage performed to identify areas with high and low water use efficiency.

Analyzing changes in GWS and irrigation water use provides valuable insights into water management practices in the study area. The irrigation efficiency data indicate significant potential for improving water use efficiency. The spatial distribution map enables the determination of areas for enhancing water management practices for sustainable agriculture.

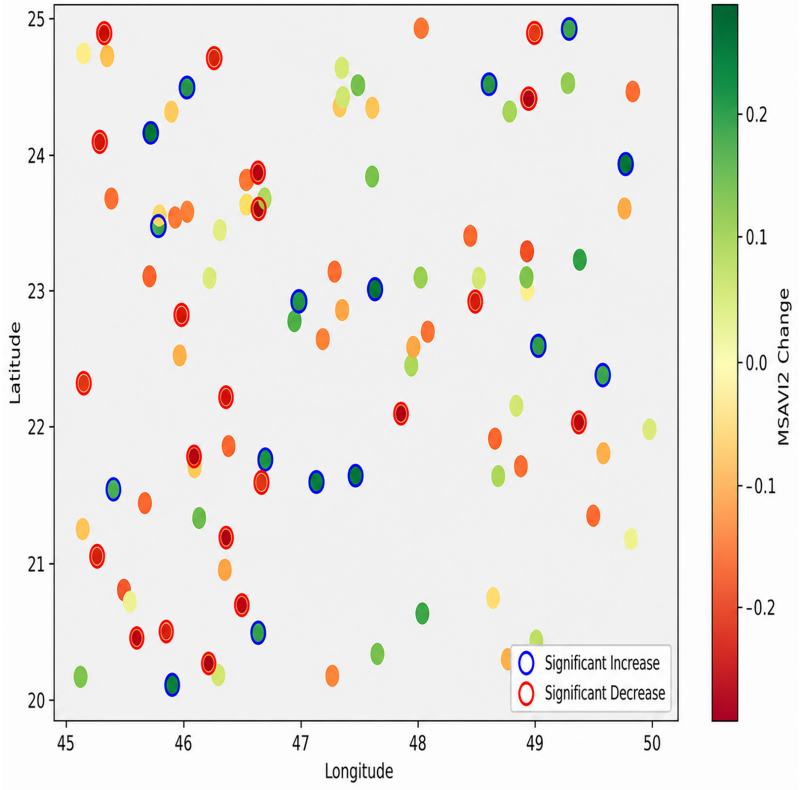


Figure 6 **Spatial distribution of MSAVI2 changes (January 2020–July 2021).**
Full-size DOI: 10.7717/peerj-cs.4071/fig-6

Table 6 **Groundwater storage changes over time.**

Time period	Mean groundwater storage (cm)	Standard deviation	Minimum storage (cm)	Maximum storage (cm)
Jan. 2020	−2.1	0.5	−3.0	−1.0
Jul. 2020	−2.8	0.6	−3.8	−1.5
Jan. 2021	−1.7	0.4	−2.5	−0.8
Jul. 2021	−2.5	0.5	−3.5	−1.3

Climatic impact on vegetation and water resources

Studying the impact of climate on vegetation and water availability is vital for improving agricultural practices. This section focuses on the effects of temperature and Rainfall on vegetation health in the study area and the GW.

To demonstrate the effect of temperature on vegetation health, we analyzed the relationship between temperature and changes in NDVI. The coefficient of temperature and NDVI over the specified periods is negative, indicating that higher temperatures are associated with lower NDVI values, as summarized in Table S3.

The relationship between monthly Rainfall and NDVI was analyzed to determine the effect of Rainfall on vegetation. From Table S4, the analysis shows a positive relationship

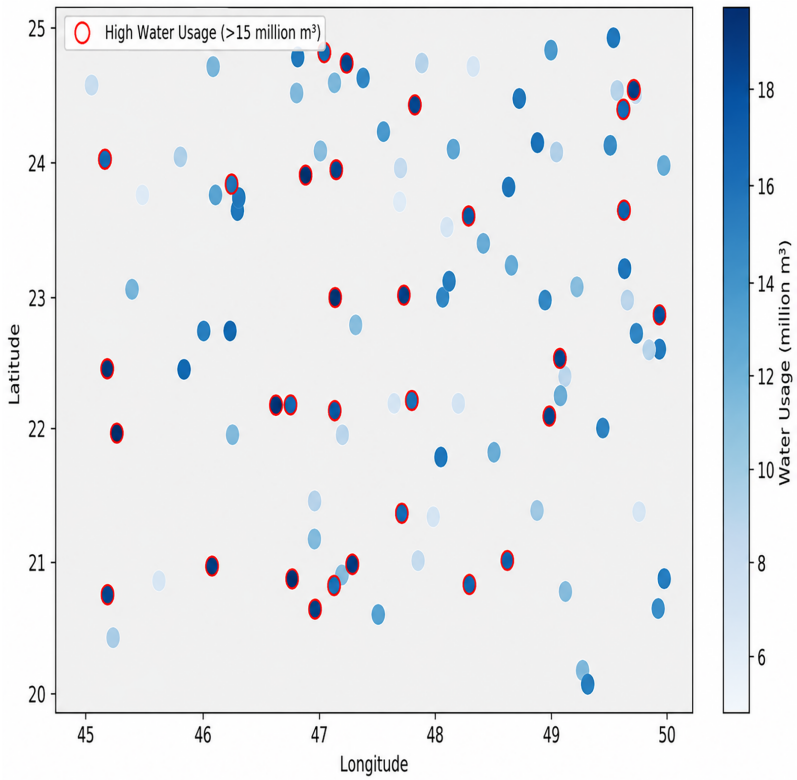


Figure 7 **Spatial distribution of water usage.** Full-size DOI: 10.7717/peerj-cs.4071/fig-7

between Rainfall and NDVI over the specified periods, which implies that as rainfall increases, NDVI also increases.

The correlation between temperature changes, temperature fluctuations, and GW levels was investigated using GRACE data.

In Table S5, we can see that the coefficients for temperature and GWS over specified periods are negative, indicating that temperature is inversely related to GWS.

The correlation between rainfall and GW levels was analyzed to determine how precipitation affects GW levels. Table S6 shows that the coefficients for rainfall and GWS for periods a and b are positive, indicating that higher Rainfall leads to higher GWS.

The study also used spatial analysis to depict the effects of temperature and Rainfall on vegetation and GWS in the study area. Spatial distribution map of areas for which significant increases in temperature reduce NDVI values, as shown in Fig. 8.

The spatial distribution of the effects of Rainfall on the change in GWS is depicted Fig. 9. Fluctuations are also marked by increased and decreased intervals, which reveal how Rainfall influences the level of GW in various regions.

Trend analysis and correlations

Identifying the relationship between agricultural and climate variables is crucial for making informed predictions and decisions. This section gives the trend analysis and

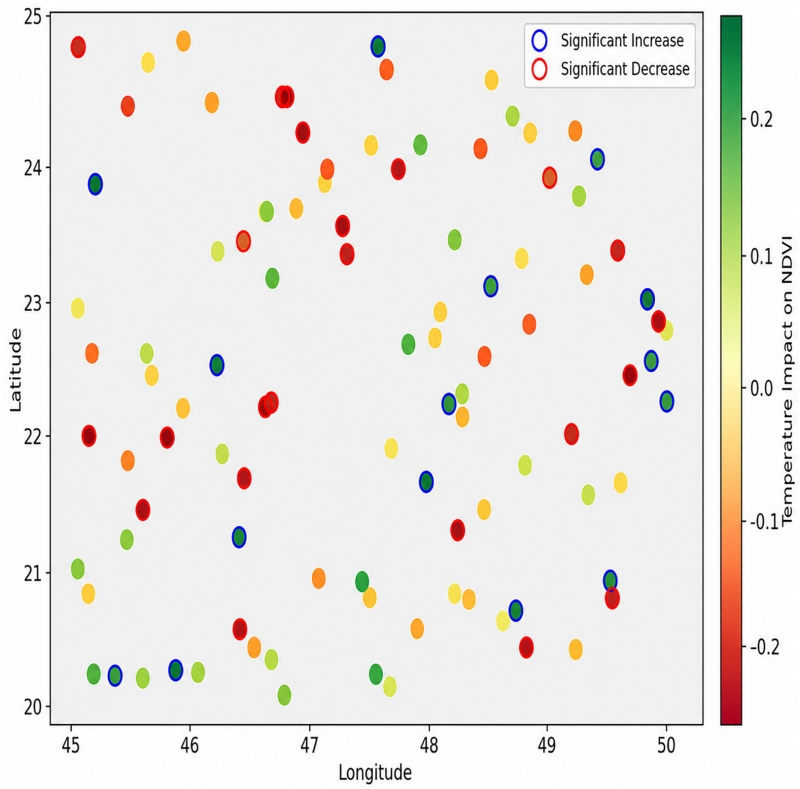


Figure 8 **Spatial distribution of temperature impact on NDVI.**
Full-size DOI: 10.7717/peerj-cs.4071/fig-8

correlation results for the study area. The trends in VIs (NDVI, SAVI, and MSAVI2) were computed over multiple years to determine long-term patterns.

Table S7 shows the trend analysis of NDVI, SAVI, and MSAVI2.

Table S8 shows the correlation coefficients (r) between VIs (NDVI, SAVI, MSAVI2) and climatic factors–temperature and Rainfall.

The negative temperature values suggest that vegetation index values decrease as temperature increases. Changes in the volume of water stored in the ground were determined using GRACE data to reveal long-term water availability. We examined the correlations between GWS and climatic variables (temperature and Rainfall). The correlation coefficients (r) between GWS and climatic variables (temperature and Rainfall) are −0.55 and 0.62.

DISCUSSION

The outcomes demonstrate that using the super resolution framework to generate the image with the SRGAN can attain a better recovery quality than bicubic interpolation and SRCNN, as demonstrated by the lower RMSE and higher PSNR and SSIM values. This enhancement helps to improve the interpretation of VIs and spatial patterns of agricultural use. Vegetation and climate analysis revealed associations at the regional scale between VIs, temperature, rain, and GWS. Vegetation conditions were negatively related to

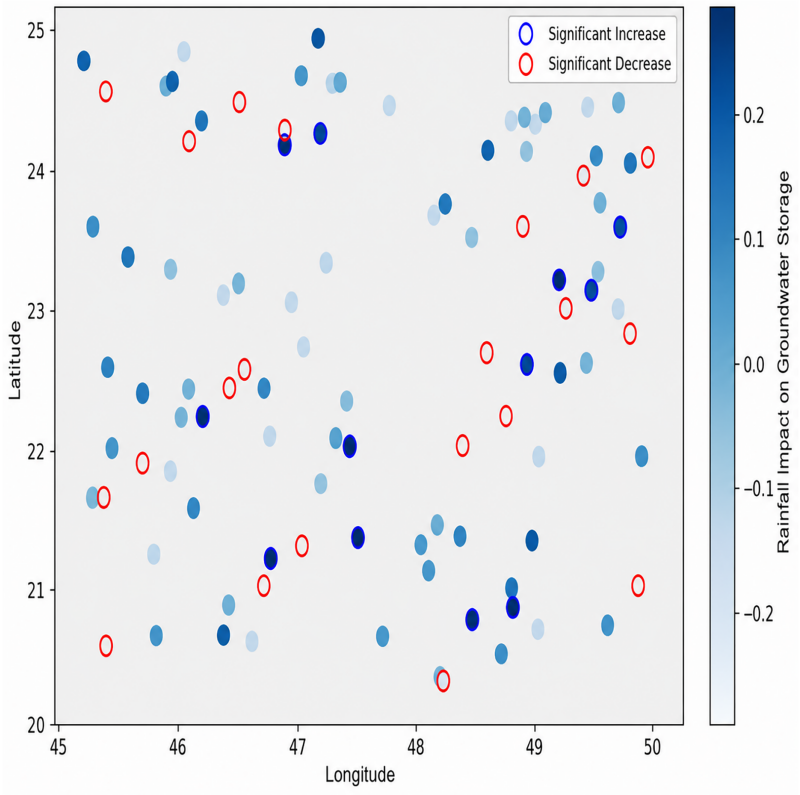


Figure 9 **Spatial distribution of rainfall impact on groundwater storage.**
Full-size DOI: 10.7717/peerj-cs.4071/fig-9

temperature, and positively related to rainfall. These relationships, however, are to be understood as regional trends and not as effects at the level of the individual pixel or as cause-and-effect relationships. In general, the results indicate that SRGAN-based super resolution can be used to monitor agriculture in water-scarce areas when combined with multisensor remote sensing and climate data, although certain constraints exist due to the study area, GRACE resolution, validation data, and computational cost.

CONCLUSION AND FUTURE WORK

This study presented an integrated multisensor remote sensing and SRGAN-based super-resolution framework for sustainable agriculture and water resource monitoring in the Al Qassim region of Saudi Arabia. The datasets of Landsat, PlanetScope, GRACE, and CRU-TS were blended to enhance images, analyze VIs, analyze GWS, and analyze regional climate correlations. Comparative results revealed that SRGAN demonstrated superior results in terms of reconstruction accuracy and structural similarity to bicubic interpolation and SRCNN, with the lowest RMSE, PSNR, and SSIM values among all the tested methods. The quality of the imagery facilitated the interpretation of the vegetation pattern spatially, and the analysis of the change in NDVI, SAVI, and MSAVI2 over time. The regional-scale climate analysis revealed that temperature negatively affected vegetation condition and that rainfall positively affected vegetation greenness.

Climate-related variability in GWS was also observed, but is constrained by the coarse spatial resolution of GRACE data. In general, the results suggest that SRGAN can be used to enhance the value of multisensor remote sensing information in agricultural monitoring in water-stressed areas. The study also includes key limitations associated with geographic scope, high-resolution reference data availability, the spatial resolution of the GRACE satellite, the necessity to perform regional-scale correlation analysis, and computational burden. The model should be expanded to other regions, more data from field validation added, and the model made more efficient, along with a study of causal relationships between climate, irrigation, vegetation condition, and GW dynamics. The results are promising; some limitations are noted. The study is geographically restricted to the Al Qassim region, Saudi Arabia, in the first place. The trained SRGAN model would therefore not necessarily be directly transferable to other arid or semi-arid agricultural areas with land cover types different from the ones that the model has been trained on, unless retrained or fine-tuned. Secondly, the native spatial resolution of the GRACE data is coarse. This can reduce the ability to detect GWS changes at the field scale and/or add smoothing effects during regional-scale interpretation of GWS changes. Third, there was a limited number of dates for which PlanetScope imagery was available. This restricts the extent of high-resolution validation and can cause a seasonal bias in the super-resolution assessment. More high-resolution reference images over several seasons would benefit model validation. Fourth, the SRGAN model was trained on a patch-based dataset created from the existing remote sensing imagery. While data augmentation was employed, the model could be further improved by increasing the size and diversity of the training set to enhance its ability to generalize and prevent overfitting. Fifth, the correlation analysis was done at the regional level based on aggregated monthly variables. As a result, the reported correlations should be understood as regional associations, and not as causal or pixel-level correlations. Irrigation date, crop species, salinity, fertilization, and management practices could affect the response by local vegetation. Sixth, data from the PME-Met-Stations were only included as additional station-level data when available. The long-term climate analysis was conducted using the CRU-TS v4.05 temperature and precipitation dataset for consistency and reproducibility. Lastly, the framework is limited in computations. The patch-based dataset and training settings were used to train the SRGAN model, which took about 18 h to complete on an NVIDIA RTX 3090 GPU. While model inference is faster than training, there is still optimization that can be made for real-time deployment, such as model pruning, patch batching, GPU-accelerated inference, or using a lighter generator architecture. The present framework is therefore not intended to be a real-time monitoring system, but rather an offline analytical framework. Future research should focus on several key areas to further enhance the understanding and application of RS in sustainable agriculture. The incorporation of other satellite and ground-based data sources can provide more accurate and comprehensive vegetation and water resource monitoring. The predictive power and decision-making processes in agriculture can be improved with the development and application of more advanced ML and DL models, such as those incorporating real-time data. It is important to undertake detailed research on the long-term effects of climate change on agricultural productivity and water availability in

order to develop adaptive strategies. More field validation and ground-truthing will help assure the reliability and accuracy of remote sensing analyses and models. High spatial and temporal resolution of remote sensing will allow even more accurate monitoring and management of agricultural practices and resources. These areas address significant challenges that could be tackled in the future to further sustainable agriculture, food security, and environmental conservation in a changing climate.

ADDITIONAL INFORMATION AND DECLARATIONS

Funding

This research is funded by the European University of Atlantic. The funders had no role in study design, data collection and analysis, decision to publish, or preparation of the manuscript.

Grant Disclosures

The following grant information was disclosed by the authors:
European University of Atlantic.

Competing Interests

The authors declare that they have no competing interests.

Author Contributions

- Abdu Salam performed the experiments, analyzed the data, performed the computation work, authored or reviewed drafts of the article, and approved the final draft.
- Fahd M. Aldosari performed the experiments, performed the computation work, authored or reviewed drafts of the article, and approved the final draft.
- Gyu Sang Choi conceived and designed the experiments, performed the experiments, analyzed the data, performed the computation work, authored or reviewed drafts of the article, and approved the final draft.
- Donia Y. Badawood performed the experiments, performed the computation work, authored or reviewed drafts of the article, and approved the final draft.
- Isabel de la Torre performed the experiments, performed the computation work, prepared figures and/or tables, authored or reviewed drafts of the article, and approved the final draft.
- Roberto Marcelo Alvarez conceived and designed the experiments, performed the experiments, performed the computation work, prepared figures and/or tables, authored or reviewed drafts of the article, and approved the final draft.
- Yini Miró performed the experiments, performed the computation work, prepared figures and/or tables, authored or reviewed drafts of the article, and approved the final draft.
- Farhan Amin performed the experiments, analyzed the data, performed the computation work, authored or reviewed drafts of the article, and approved the final draft.

Data Availability

The following information was supplied regarding data availability:

The data is available in the Supplemental Files.

The code is available at Zenodo: Amin, F. (2026). Development of a Novel Machine Learning Framework for Sustainable Agricultural Development [Computer software]. Zenodo. https://doi.org/10.5281/zenodo.21053153.

The Landsat Collection 2 Level 2 data is available at: https://www.usgs.gov/landsat-missions/landsat-collection-2-level-2-science-products.

The GRACE TWS data is available at: https://www.eoportal.org/satellite-missions/grace.

The PlanetScope data is available at: https://earth.esa.int/eogateway/missions/planetscope.

The CRU-TS v4.05 is available at Figshare: Team, Scientific Data Curation (2020). Metadata record for: Version 4 of the CRU-TS monthly high-resolution gridded multivariate climate dataset. figshare. Dataset. https://doi.org/10.6084/m9.figshare.11980500.v1.

The PME Met Station records are available at: https://datasource.kapsarc.org/explore/dataset/average-atmospheric-pressure-in-hpmb-observed-by-pme-met-stations-2009xls0/information/.

Supplemental Information

Supplemental information for this article can be found online at http://dx.doi.org/10.7717/peerj-cs.4071#supplemental-information.

REFERENCES

Alsubaie MG, Luo S, Shaukat K, Zhang W. 2026. A novel Alzheimer's disease classification framework integrating 3D CNN with bidirectional feature pyramid network and vision transformers. *IEEE Access* **14(2)**:15241–15259 DOI 10.1109/access.2026.3658311.

Altieri MA, Nicholls CI, Henao A, Lana MA. 2015. Agroecology and the design of climate change-resilient farming systems. *Agronomy for Sustainable Development* **35**:869–890 DOI 10.1007/s13593-015-0285-2.

Barman T, Deka B, Mullah HU. 2023. Edge-preserving single remote-sensing image super-resolution using sparse representations. *SN Computer Science* **4(3)**:312 DOI 10.1007/s42979-023-01764-7.

Beegum S, Reddy KR, Ambinakudige S, Reddy V. 2024. Planting for perfection: how to maximize cotton fiber quality with the right planting dates in the face of climate change. *Field Crops Research* **315**:109483 DOI 10.1016/j.fcr.2024.109483.

Botero-Valencia J, García-Pineda V, Valencia-Arias A, Valencia J, Reyes-Vera E, Mejia-Herrera M. 2025. Machine learning in sustainable agriculture: systematic review and research perspectives. *Agriculture* **15(4)**:377 DOI 10.3390/agriculture15040377.

Chakraborty T, Reddy KSU, Naik SM, Panja M, Manvitha B. 2024. Ten years of generative adversarial nets (GANs): a survey of the state-of-the-art. *Machine Learning: Science and Technology* **5(1)**:011001 DOI 10.1088/2632-2153/ad1f77.

Choi E, Choi J, Kang MG. 2004. Super-resolution approach to overcome physical limitations of imaging sensors: an overview. *International Journal of Imaging Systems and Technology* **14(2)**:36–46 DOI 10.1002/ima.20006.

Di L, Yu E. 2023. Remote sensing. In: *Remote Sensing Big Data*. Cham: Springer, 17–43.

Flora CB. 2010. Food security in the context of energy and resource depletion: sustainable agriculture in developing countries. *Renewable Agriculture and Food Systems* **25**:118–128 DOI 10.1017/S1742170510000177.

Gebbers R, Adamchuk VI. 2010. Precision agriculture and food security. *Science* **327(5967)**:828–831 DOI 10.1126/science.1183899.

Govender M, Chetty K, Naiken V, Bulcock H. 2008. A comparison of satellite hyperspectral and multispectral remote sensing imagery for improved classification and mapping of vegetation. *Water SA* **34(2)**:147–154 DOI 10.4314/wsa.v34i2.183634.

Haq MA. 2024. Intelligent sustainable agricultural water practice using multisensor spatiotemporal evolution. *Environmental Technology* **45(12)**:2285–2298 DOI 10.1080/09593330.2021.2005151.

Haring S, Gaudin AC, Hanson BD. 2023. Functionally diverse cover crops support ecological weed management in orchard cropping systems. *Renewable Agriculture and Food Systems* **38**:e54 DOI 10.1017/s1742170523000492.

Harris I, Osborn TJ, Jones P. 2020. Version 4 of the climate research unit time-series (CRU-TS) monthly high-resolution gridded multivariate climate dataset. *Scientific Data* **7**:109 DOI 10.1038/s41597-020-0453-3.

He H, Chen T, Chen M, Li D, Cheng P. 2019. Remote sensing image super-resolution using deep–shallow cascaded convolutional neural networks. *Sensor Review* **39(5)**:629–635 DOI 10.1108/sr-11-2018-0301.

Hobbs PR, Sayre K, Gupta R. 2008. The role of conservation agriculture in sustainable agriculture. *Philosophical Transactions of the Royal Society B: Biological Sciences* **363**:543–555 DOI 10.1098/rstb.2007.2169.

Jackson RD, Idso S, Reginato R, Pinter P Jr. 1981. Canopy temperature as a crop water stress indicator. *Water Resources Research* **17(4)**:1133–1138 DOI 10.1029/wr017i004p01133.

Jayabal R. 2025. Next-generation solutions for water sustainability in nuclear power plants: innovations and challenges. *Nuclear Engineering and Design* **432(3)**:113757 DOI 10.1016/j.nucengdes.2024.113757.

Jin D, Pan Y, Brandt M, Fan L, Zhu Y, Qi W, Huang H, Wang Q, Shi P, Qi J. 2026. AI-based 2-m super-resolution of Sentinel-2 imagery for high-resolution SDG monitoring. *GIScience & Remote Sensing* **63(1)**:2640266 DOI 10.1080/15481603.2026.2640266.

Jose S. 2009. *Agroforestry for ecosystem services and environmental benefits: an overview*. Cham: Springer.

KAPSARC. 2024. PME met station, general authority for statistics, KAPSARC data portal. *Available at https://datasource.kapsarc.org/explore/dataset/average-atmospheric-pressure-in-hpmb-observed-by-pme-met-stations-2009xls0/information/*.

Kramer DH. 2022. Gravity recovery and climate experiment (GRACE). *Available at https://www.eoportal.org/satellite-missions/grace*.

Kwon DH, Hong SM, Abbas A, Park S, Nam G, Yoo JH, Kim K, Kim HT, Pyo J, Cho KH. 2023. Deep learning-based super-resolution for harmful algal bloom monitoring of inland water. *GIScience & Remote Sensing* **60(1)**:2249753 DOI 10.1080/15481603.2023.2249753.

Li J, Meng Y, Tao C, Zhang Z, Yang X, Wang Z. 2023. ConvFormerSR: fusing transformers and convolutional neural networks for cross-sensor remote sensing imagery super-resolution. *IEEE Transactions on Geoscience and Remote Sensing* **62(1)**:1–15 DOI 10.1109/tgrs.2023.3340043.

Liebel L, Körner M. 2016. Single-image super resolution for multispectral remote sensing data using convolutional neural networks. In: *The International Archives of the Photogrammetry, Remote Sensing and Spatial Information Sciences*. Vol. 41, 883–890.

Ma S, Zhuge M. 2024. Ecological agriculture traits: constructing an integrated agricultural system for sustainable development. *Geographical Research Bulletin* **3**:2–5 DOI 10.50908/grb.3.0_2.

Neyns R, Canters F. 2022. Mapping of urban vegetation with high-resolution remote sensing: a review. *Remote Sensing* **14(4)**:1031 DOI 10.3390/rs14041031.

Onstad DW, Knolhoff LM. 2023. Major issues in insect resistance management. In: *Insect Resistance Management*. Amsterdam: Elsevier, 1–29.

Park SC, Park MK, Kang MG. 2003. Super-resolution image reconstruction: a technical overview. *IEEE Signal Processing Magazine* **20**:21–36 DOI 10.1109/MSP.2003.1203207.

Pinter PJ Jr, Hatfield JL, Schepers JS, Barnes EM, Moran MS, Daughtry CS. 2003. Remote sensing for crop management. *Photogrammetric Engineering & Remote Sensing* **69(6)**:647–664 DOI 10.14358/pers.69.6.647.

PlanetScope DATA. 2024. European space agency. *Available at https://earth.esa.int/eogateway/missions/planetscope*.

Raihan A. 2024. A systematic review of geographic information systems (GIS) in agriculture for evidence-based decision making and sustainability. *Global Sustainability Research* **3(1)**:1–24 DOI 10.56556/gssr.v3i1.636.

Raj R, Kar S, Nandan R, Jagarlapudi A. 2020. Precision agriculture and unmanned aerial Vehicles (UAVs). In: *Unmanned Aerial Vehicle: Applications in Agriculture and Environment*. Cham: Springer International Publishing, 7–23 DOI 10.1007/978-3-030-27157-2_2.

Ran Q, Xu X, Zhao S, Li W, Du Q. 2020. Remote sensing images super-resolution with deep convolution networks. *Multimedia Tools and Applications* **79(13–14)**:8985–9001 DOI 10.1007/s11042-018-7091-1.

Reganold JP, Wachter JM. 2016. Organic agriculture in the twenty-first century. *Nature Plants* **2**:15221 DOI 10.1038/nplants.2015.221.

Riaz R, Han G, Shaukat K, Khan NU, Zhu H, Wang L. 2025. A novel ensemble Wasserstein GAN framework for effective anomaly detection in industrial internet of things environments. *Scientific Reports* **15(1)**:26786 DOI 10.1038/s41598-025-07533-1.

Sumith N, Rashmi M. 2026. A systematic review of deep learning and super resolution techniques for leaf-level and canopy-level plant disease detection. *Discover Artificial Intelligence* **6(1)**:8812019 DOI 10.1007/s44163-026-00973-2.

Thenkabail PS, Smith RB, Pauw ED. 2000. Hyperspectral vegetation indices and their relationships with agricultural crop characteristics. *Remote Sensing of Environment* **71(2)**:158–182 DOI 10.1016/s0034-4257(99)00067-x.

Vasilescu V, Datcu M, Faur D. 2023. A CNN-based sentinel-2 image super-resolution method using multiobjective training. *IEEE Transactions on Geoscience and Remote Sensing* **61(6)**:1–14 DOI 10.1109/tgrs.2023.3240296.

Wang L, Liu L, Yu Q, Yuan D. 2026. Generative adversarial network-based super-resolution reconstruction of remote sensing images. *Scientific Reports* **16**:11971 DOI 10.1038/s41598-026-41832-5.

Wang Z, Menenti M. 2021. Challenges and opportunities in Lidar remote sensing. *Frontiers in Remote Sensing* **2**:641723 DOI 10.3389/frsen.2021.641723.

Wu H, Li Z-L. 2009. Scale issues in remote sensing: a review on analysis, processing and modeling. *Sensors* **9**:1768–1793 DOI 10.3390/s90301768.

Yang J, Ren H, He Z, Zeng M. 2026. Deep learning-based remote sensing image super-resolution: recent advances and challenges. *Neurocomputing* **674**:132939 DOI 10.1016/j.neucom.2026.132939.

Yateh M, Li C, Li F, Gu C, Ma S, Lu B. 2025. Understanding the influence of energy and chemical use on water treatment plants carbon emissions accounting. *Journal of Water Process Engineering* **69(21)**:106669 DOI 10.1016/j.jwpe.2024.106669.

Zhu XX, Tuia D, Mou L, Xia G-S, Zhang L, Xu F. 2017. Deep learning in remote sensing: a comprehensive review and list of resources. *IEEE Geoscience and Remote Sensing Magazine* **5**:8–36 DOI 10.1109/MGRS.2017.2762307.